THESIS FOR THE DEGREE OF LICENTIATE OF ENGINEERING

Polysaccharide thin film studies

Adsorption of oxidized xylan on cellulose

CHONNIPA PALASINGH

Department of Chemistry and Chemical Engineering

CHALMERS UNIVERSITY OF TECHNOLOGY

Gothenburg, Sweden 2021

Polysaccharide thin film studies
Adsorption of oxidized xylan on cellulose

CHONNIPA PALASINGH

Technical report no 2021:06

Department of Chemistry and Chemical Engineering
Chalmers University of Technology
SE-412 96 Gothenburg
Sweden
Telephone +46 (0)31-772-1000

Cover: Adsorption of wood oxidized xylan on cellulose thin film.

Printed by Chalmers Reproservice
Gothenburg, Sweden 2021

Polysaccharide thin film studies

Adsorption of oxidized xylan on cellulose

CHONNIPA PALASINGH
Department of Chemical and Chemistry Engineering
Chalmers University of Technology

Abstract

Wood xylans are renewable natural materials that have potential for future use in bio-based products. However, their high price and low production capacity restrict their industrial use and current applications. This research aimed to explore the potential of wood xylans for film applications. Most xylans extracted from wood do not dissolve in water, which is a common solvent in many industries, such as the pulp and paper industry. Furthermore, bio-based materials are expected to be processed in a green approach, where water is a preferable solvent, and has benefit in terms of low-cost, and being an environmentally benign solvent. The poor water interaction of xylans hinders dissolution and film production, but can be overcome by chemical modification of xylan to alter its properties. Regioselective oxidation—a well-known modification in polysaccharides—can increase the flexibility and water interaction of xylans by opening their monosaccharide ring and equipping them with aldehyde groups. The research employed quartz crystal microbalance with dissipation monitoring (QCM-D) and surface plasmon resonance (SPR) to study the adsorption of macromolecules on film surfaces. The analytical combination was first established for studying protein adsorption on cellulose film with different morphology, and structure, and then oxidized xylan adsorption on nanocellulose films, which was the focus of this research. The influence of the molecular weight of oxidized xylan on adsorption in aqueous conditions, and its effect on film swelling were explored. The behavior of oxidized xylan in solution was observed using dynamic light scattering, showing that high molecular weight oxidized xylan formed larger aggregates when the concentration increased compared to low molecular weight oxidized xylan. The QCM-D and SPR investigations revealed that a high molecular weight grade adsorbed preferentially on a neutral cellulose surface, while both grades were adsorbed independently of molecular weight on a negatively charged surface. The impact of oxidized xylan on the swelling of cellulose films, regardless of molecular weight, was due to oxidized xylan bringing more water to the non-charged films, while the opposite was true of negatively charged films. Also, applying the combination of QCM-D and SPR techniques to oxidized xylan adsorption on cellulose, water content and adsorbed dry mass were obtained. This study provides a stepping-stone toward the future use of bio-based materials obtained from forest sources.

Keywords: solubility, quartz crystal microbalance with dissipation monitoring, QCM-D, surface plasmon resonance, SPR, macromolecule adsorption

Published Papers

I. **Design of Friction, Morphology, Wetting, and Protein Affinity by Cellulose Blend Thin Film Composition.**

Caterina Czibula; Gundula Teichert; Maximilian Nau; Mathias Hobisch, **Chonnipa Palasingh**, Markus Biesalski, Stefan Spirk, Christian Teichert, and Tiina Nypelö.

Frontiers in Chemistry 7(2019), article number: 239.

II. **Oxidized xylan additive for nanocellulose films—a swelling modifier.**

Chonnipa Palasingh; Anna Ström; Hassan Amer; and Tiina Nypelö.

International Journal of Biological Macromolecules 180(2021): 753–759.

Author Contributions

I. Co-performed quartz crystal microbalance with dissipation monitoring experiments. Co-author.

II. Planned experiments with the coauthors, performed all experiments, and wrote the manuscript with support from coauthors. Main author.

Abbreviations

CNFs	Cellulose nanofibers
DLS	Dynamic light scattering
DO	Degree of oxidation
HX	High molecular weight oxidized xylan
LX	Low molecular weight oxidized xylan
PBS	Phosphate buffer solution
QCM-D	Quartz crystal microbalance with dissipation monitoring
SPR	Surface plasmon resonance
TCNFs	TEMPO oxidized cellulose nanofibers

Contents

1. Introduction

Materials and energy today mainly originate from fossil oil, coal, and natural gases. Increasing demand as the world population has expanded has led to increased awareness of resource shortages and their environmental impacts, yet demand and consumption continue to increase. The development of alternative materials from renewable and natural resources provides an opportunity to help decrease the environmental impacts of such demand, driving research on sustainable materials and technology.

Wood materials have long played an important role in human civilization. They have been used to provide heat, make tools, and construct furniture, shelters, and infrastructures. As manufacturing technologies developed, wood was processed into fibers, and its use expanded to paper manufacturing. In the nineteenth century, a modern pulping process for wood was established.[1] The process involved three main molecular products: cellulose, hemicellulose, and lignin. These products can be used as monomer building blocks for chemicals and materials, or as polymers for a variety of applications. Cellulose is used in paper products, textiles, food, pharmaceuticals, hygiene products, cosmetics, and medical materials. Lignins are incinerated to produce energy but can also be converted into valuable products: carbon fibers, fine chemicals, and phenol derivatives.[2] However, development and innovations in the use of wood hemicelluloses are limited compared to those for cellulose and lignin. Hemicelluloses from agricultural sources (e.g., corn, wheat, rye, and barley) are used in materials engineering for films, coatings, additives, and stabilizers [3], and hemicelluloses from guar gum and locust bean gum are used in the food, cosmetics, and pharmaceutical industries.[4-6] Nevertheless, wood-based hemicelluloses are rarely used in materials engineering, perhaps due to a lack of effective extraction and purification technology and low cost-efficiency. Furthermore, the extracted products are used in limited applications. Hemicelluloses could, however, be utilized in materials engineering as an extracted product or as part of cellulose fiber products. The interest in the addition of hemicelluloses to cellulose materials has been motivated by the circular economy and the use of forest-based additives for new properties. Hemicelluloses that are bound to wood fibers have an implication to their strength and flexibility. [7-9] The presence of hemicellulose in cellulose fibers affects the amount of water in film, its removal (dewatering), and the energy required for fiber disintegration for papermaking purposes. Consequently, hemicelluloses have been demonstrated as hydration modifiers for cellulose nanofibrils, contributing to their viscoelastic properties with extended utilization by varying pH and salt concentrations.[10] The use of hemicelluloses for film applications has been a topic of many studies.[11-16] Adsorptive modification of cellulose films by hemicelluloses is facile and has been reported for xylans,[17] acetylated xylans,[18] arabinoxylans,[19-21] xyloglucans,[22] and glucuronoxylans.[8, 23]

This research explored the utilization of macromolecules in materials engineering. The focus was on wood xylans and unraveling their potential for film applications. We hypothesized that solvent interactions would be an underlying challenge for xylan polymer utilization. Most xylan polymer extracts from wood do not dissolve in water, although water is a common solvent used in the pulp and paper industry; an important stakeholder in hemicellulose research. Modification is a means to overcome this obstacle and change xylan solubility. Oxidation was chosen as a method to increase the water solubility of xylan in this research. Periodate oxidation regioselectively cleaves the bond between carbons in position 2 and 3 of monosaccharide units. A previous study showed that oxidized xylan is rendered into a hemialdal-rich structure that differs from the closed ring structure of unoxidized xylan.[24] We developed an analytical approach that combined two surface-sensitive techniques to study marcromolecule adsorption on polysaccharide surfaces. The approach

was demonstrated first by studying polymer adsorption and then used as the focus of the research to investigate the properties of oxidized xylan in solution and its influence on polysaccharide films.

2. Background

2.1 Wood polysaccharides

Polysaccharides are the main components of wood cell walls. They can be either homopolysaccharides or heteropolysaccharides and are linear or branched in structure. Wood cell walls are composed of cellulose, hemicelluloses, and lignin.[1] The first two components are polysaccharides, while the third is a class of aromatic compounds. The proportion of cell wall components depends on cell type and plant species. In general, wood cell walls consist of a layer of primary cell wall and three layers of secondary cell wall. Each layer has a distinct chemical composition and thickness. Monosaccharides are the smallest repeating units; they covalently bind to other monosaccharides through condensation of hydroxyl groups (so-called glycosidic bonds) to form di-, tri-, oligo-, and polysaccharides. Common monosaccharides found in plant cell walls are pentoses (xylose and arabinose) and hexoses (glucose, mannose, and galactose; see Figure 1). Xylose, glucose, and mannose are typical backbone units, while arabinose and galactose are present as substituting units attached to the backbone units. Moreover, uronic acids and acetyl groups are often present as substituents.[25]

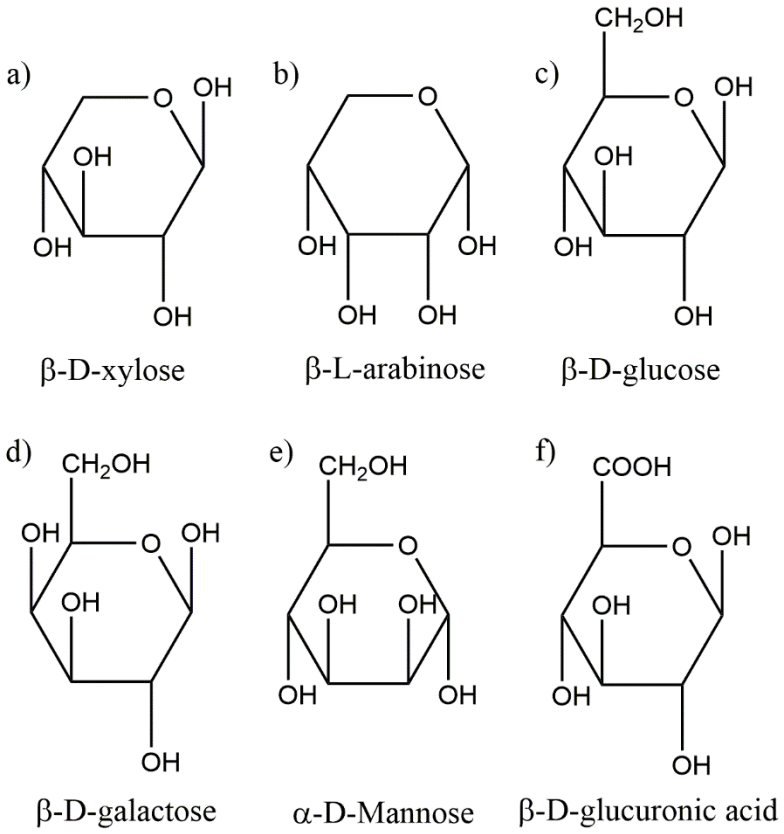

Figure 1. Haworth projections for common monosaccharides in wood: xylose (a), arabinose (b), glucose (c), galactose (d), mannose (e), and glucuronic acid (f).

2.1.1 Cellulose

Cellulose is the most abundant polysaccharide in plant cell walls. It is a linear homopolysaccharide composed of β-D-glucopyranose units that link with β-1,4-glycosidic bonds.

Around 40–45 % of cellulose is found in wood species.[26] Wood cellulose is organized into fibrils, which are controlled by biosynthesis.[27] Different orientations of cellulose microfibrils in plant cell wall layers govern the physical properties of plant cells and wood. Such fibrils are referred to as microfibrils or elementary fibrils.

Wood or wood pulp can be exposed to treatments that aim to liberate the cellulose fibrils for materials engineering purposes. The fibrils are generally produced using high shear mechanical treatments (e.g., homogenization and grinding). Biological and chemical pretreatments are used to enhance fibrillation and reduce energy consumption, which may influence surface chemistry; for instance, a negatively charged cellulose product is generated when 2,2,6,6-tetramethylpiperidine-N-oxyl (TEMPO) oxidation is used as the pretreatment to improve delamination during defibrillation.[28] The fibril grades are referred to as nano- and microfibrillated celluloses, or nano- and microfibrils. The chosen name generally depends on the size of the units, whether the material comprises liberated fibrils or fibrillated surfaces, and the historical context. Here, we refer to these grades as nanocelluloses. The properties of nanocelluloses depend on their origins and extraction processes. Cellulose nanofibers (CNFs) comprise ordered and disordered regions. In materials engineering, CNFs have the advantages of low densities, high aspect ratios, large surface areas, and abundant hydroxyl groups, which facilitate various chemical modifications.[29]

Transparent nanocellulose films are being developed as new-generation film materials.[30, 31] Nanocellulose films can be made by dispersing cellulose fibrils in water and evaporating the solvent. This method forms films, and the films' appearance resembles that of plastic films; however, the film properties are inferior to those of plastic, especially regarding humidity sensitivity. Since cellulose is hydrophilic, the film is hygroscopic, which results in poor properties in highly humid environments. The moisture causes nanocellulose to swell and change its network structure. The swelling occurs in the amorphous region and the fibril outer surface on which water molecules can access. Swelling behavior is governed by various parameters, such as crystallinity, degree of polymerization (DP), degree of substitution, and solvent properties, which influence fiber-solvent interaction. However, cellulose fiber or film maintains its structure despite increasing volume due to solvent uptake and changes in its physical network structure.[32]

2.1.2 Hemicelluloses

Hemicelluloses are found in the matrix between cellulose microfibrils in cell walls, constituting approximately 20–35 % of the total mass.[33] A variety of monosaccharides, such as glucose, mannose, galactose, xylose, and arabinose with small amounts of uronic acids and other deoxyhexoses, are found in hemicelluloses. Extracted homo- or heteropolysaccharide hemicelluloses are diverse in structure, chemical composition, and size, depending on the plant species and extraction method used.

Xylan is a linear homopolysaccharide composed mainly of β-D-xylopyranose units linked by β-1,4-glycosidic bonds with some uronic acid side groups. Hardwoods contain 10–35 % xylan, while only 10–15 % is found in softwoods. Softwood xylan tends to contain more uronic acids and exhibits an absence of an acetyl group compared to hardwood xylan. Furthermore, arabinose side groups have been found as substituents in softwoods.[33, 34]

2.2 Solubility of xylans

The solubility of xylan is influenced by its structure, molecular weight, and inter-/intra molecular bonding. The xylan structure and molecular weight in nature depend on the species of wood; for example, hardwood xylan contains approximately 10–15 wt/% of acetyl and has an average molecular weight of around 5,600–40,000 g/mol.[35-37] Furthermore, the side group

substituents influence the stability of xylan and prevent depolymerization during extraction. Uronic acids in hardwoods stabilize xylan during kraft pulping, while arabinose side groups stabilize softwood xylan during alkali extraction.[38] The degree of substitution in these groups is decisive for their water solubility. Increasing acetylation leads to solubility in aprotic solvents.[39] Side chains such as arabinose and glucuronic acids and their distribution patterns influence not only solubility but behavior in solution, interaction with other molecules, and chemical and enzyme modifications.

Water is a target solvent for many applications benefiting from renewable materials; hence, water solubility is desirable. Xylan is not soluble in water in its native form, but short xylans (DP < 30) may dissolve in water.[40] High-DP xylans have the advantage of containing many hydroxyl groups and having long backbone chains, which are beneficial for film formation and enhance film properties. Chemical or enzyme modification is required to change xylan structure and increase water solubility. Xylan has abundant in hydroxyl groups, facilitating such modifications. The issue of water solubility has been tackled by etherification in modification to derive hydroxypropylated xylan and further alkylated grades.[41] Furthermore, oxidation of xylans is a method for changing a structure of xylan and altering their properties. Oxidation via periodate is a well-known modification of carbohydrates for structural analysis in carbohydrate chemistry [42] and is a prominent modification method used in materials engineering.

2.3 Oxidation of xylan

During chemical modification of polysaccharides using sodium periodate, periodate ions attack hydroxyl groups regioselectively at the diol structure (C2 and C3) of xylose units and form reactive aldehydes (Figure 2). During oxidation, newly created aldehydes partly convert to hydrated aldehyde and/or form hemiacetal or hemialdal bridges in the presence of water. Such conversions are partially reversible and they can be converted back into free aldehydes in a dry state.[43] The water solubility of xylan increases following oxidation,[24] perhaps due to increased water interaction, because the opened rings facilitate a more flexible backbone structure, or because oxidation reduces the molecular weight. Furthermore, the aldehydes may act as intermediates for further grafting or reduce to a more stable form as alcohol.

Oxidation has the drawback of decreasing the degree of polymerization of xylan. A peeling reaction at the reducing end and random attacks by hydroxyl radicals created from the decomposition of periodate ions are the main causes of xylan depolymerization. This can be mitigated to some extent by the addition of isopropanol during oxidation.[44]

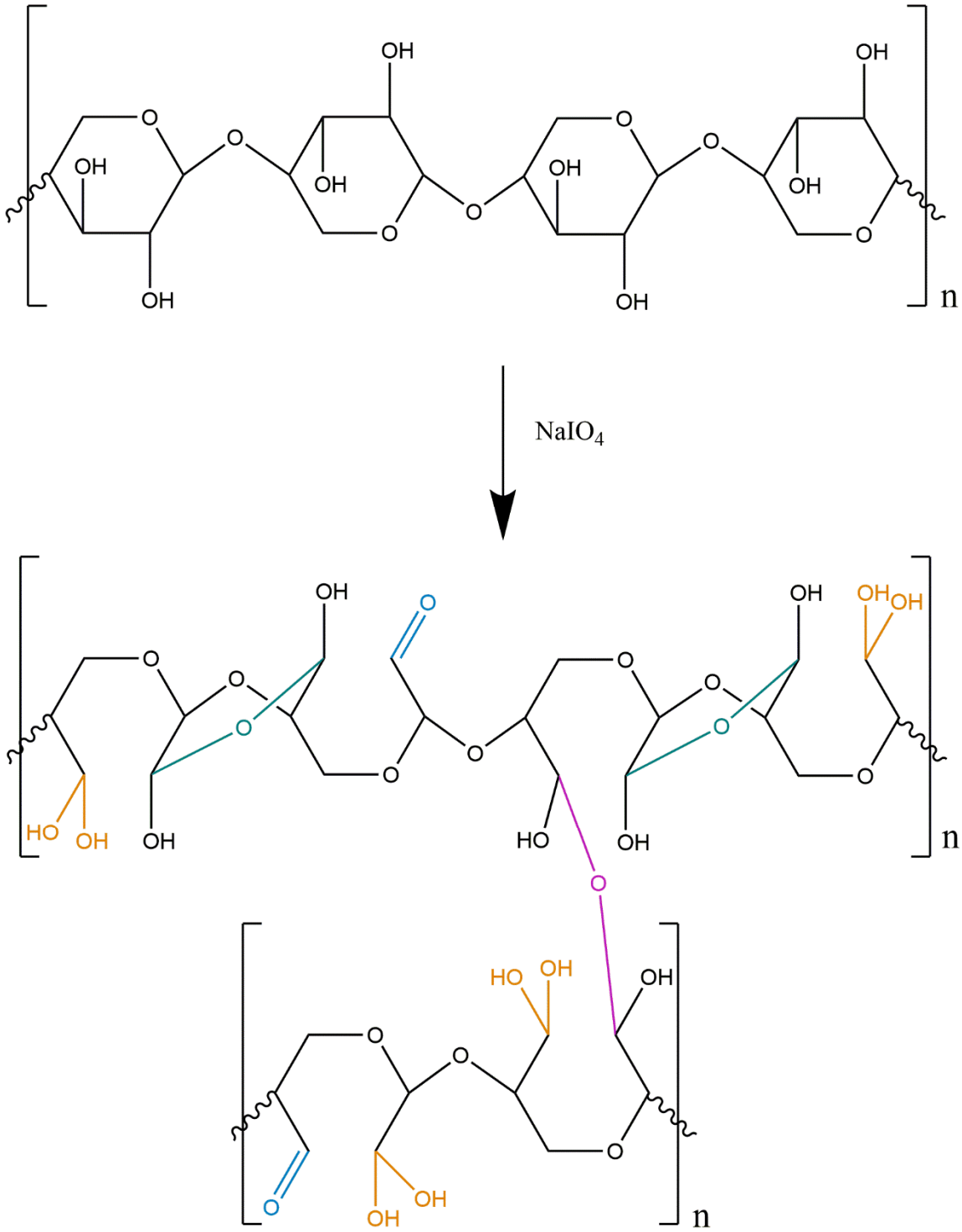

Figure 2. Periodate oxidation of xylan and possible conformations of oxidized xylan: free aldehyde (blue), hydrated aldehyde (orange), intra-hemialdal linkage (green), and inter-hemialdal linkage (magenta).

There are concerns about the use of periodate oxidation for producing materials, since large amounts of periodate are needed and periodate is both toxic (LD50 value 58 mg/kg) [45] and expensive. Process development for periodate regeneration has focused on minimizing the use of

periodate and increasing cost efficiency. The regeneration of periodate in cellulose oxidation has been shown to decrease the cost of oxidation from 16,500 €/ton to around 450 €/ton.[46] Development of regeneration procedures [47] is paramount for engineering use,[43] but was not the focus of this research.

2.4 Surface sensitive techniques

The analysis in this study focused on phenomena occurring on the surfaces of polysaccharide films. The analytical approach employed surface-sensitive techniques. Quartz crystal microbalance with dissipation monitoring (QCM-D) and surface plasmon resonance (SPR) are real-time monitoring and label-free surface-sensitive techniques with nanoscale resolution. These two techniques are complementary because they probe the same phenomenon at the same length scale; however, they detect different physical phenomena and hence enable complementary information to be gathered.

2.4.1 Quartz crystal microbalance with dissipation monitoring

QCM-D detects the mass and viscoelastic properties of a film or layer bound onto a substrate. In principle, a sensor is excited and resonates in response to applied voltage. A resonance frequency is monitored as a function of time, and the frequency changes due to changes in mass when a substance is coupled to the sensor (Figure 3). This phenomenon can be used for adsorption or desorption studies. At the same time with frequency change (Δf), dissipation (D) or energy loss is measured by recording the amplitude of the oscillation as a function of time when withdrawing the voltage. The value of D represents the rigidity of a layer; for example, dissipation increases when a layer swells and decreases when a layer collapses. A combination of Δf and D facilitates understanding of the adsorbed mass and its viscoelasticity.

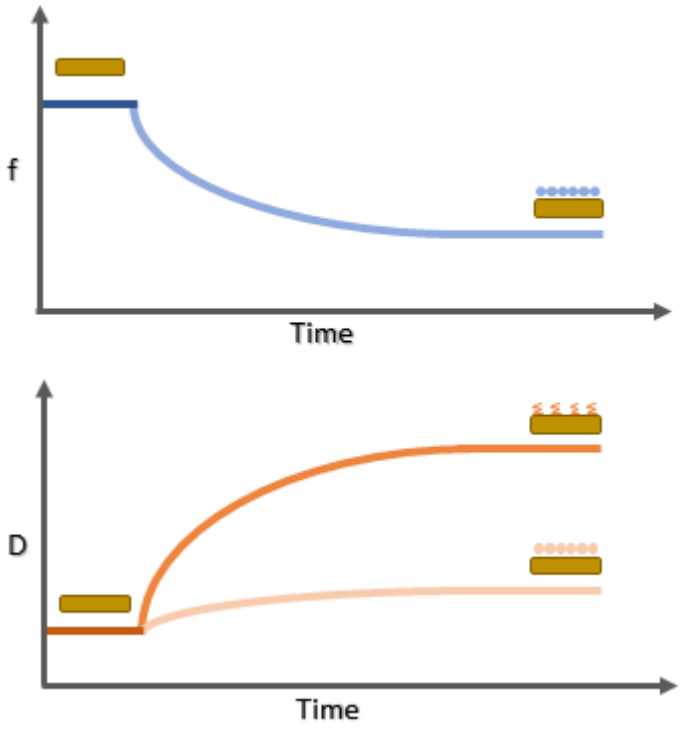

Figure 3. Illustration of a resonance frequency decreased due to mass adsorbed on the surface (top) and a dissipation change due to different molecules adsorbed on the surface (bottom).

2.4.2 Surface plasmon resonance

The surface plasmon phenomenon occurs when polarized light hits a metal film, causing electrons on the metal film to oscillate and adsorb light. The Kretschmann configuration is a common configuration used in SPR (Figure 4), whereby polarized light travels through a prism onto the metal film on the SPR sensor and is reflected to a light detector. The total internal reflection (TIR) angle is the angle at which a metal layer acts like a perfect mirror and reflects all the light back to the detector. The TIR value depends on the bulk refractive index of the medium, which is in contact with the surface. On the other hand, the minimum intensity angle is an incident angle at which most of the light is adsorbed through the plasmon phenomenon and almost no light is reflected to the detector. The detection range of SPR lies within an electromagnetic field (evanescent region) that extends a few hundred nanometers from the metal surface in a perpendicular direction.[48] When molecules adsorb on the surface, the refractive index of the surface changes, which results in a shift at a minimum intensity angle (Figure 4). For angular scanning, SPR is used to observe the intensity of the refracted light as a function of the incident angle. With continuous angular scanning, SPR can observe real-time kinetic adsorption or desorption through a change in the minimum intensity angle as a function of time.

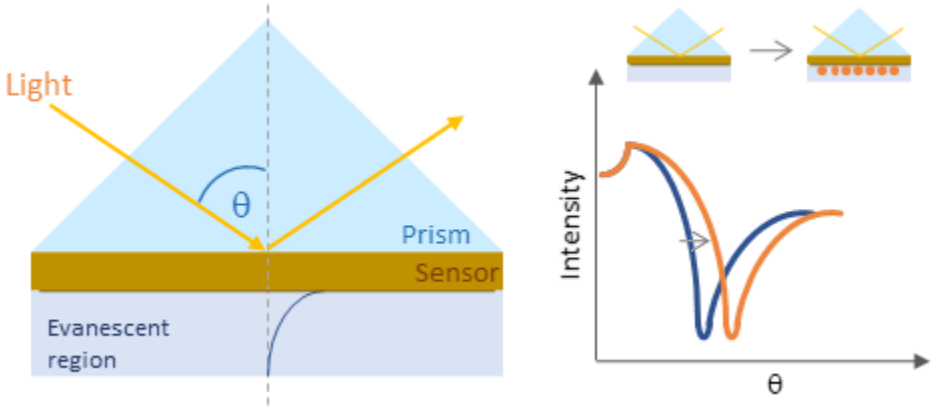

Figure 4. SPR in the Kretschmann conformation (left) and angular scans with the minimum intensity angle shifted from its original position (blue curve) as a result of molecules adsorbed on a surface (right).

3. Materials and Methods

Chemicals were purchased from Sigma Aldrich and used without further purification unless otherwise stated. Xylan from beech wood (low molecular weight) and birch wood (high molecular weight) were oxidized with sodium periodate ($NaIO_4$) prior to the study, according to Amer et al. [24] In brief, 20 g of xylan was suspended in 1.6 l of periodate solution, which contained 35 g of $NaIO_4$. The reaction was performed with an absence of light on a shaker for 96 h. The reaction was observed using ultraviolet-visible (UV-Vis) spectroscopy to monitor the concentration of periodate in a suspension at 290 nm.[49] The oxidized xylan was purified with dialysis for 2 d and then lyophilized. The degree of oxidation (DO) was 91.7 % and 91.6 % for LX and HX, respectively, determined from the UV absorbance at 290 nm. Molecular weight reduced from 7,700 g/mol to 5,070 g/mol for LX and from 31,000 g/mol to 12,600 g/mol for HX according to gel permeation chromatography in dimethyl sulfoxide (DMSO). Xylan from beech wood (Megazyme) was used for preliminary studies to control the DO.

CNFs were obtained from softwood kraft pulp. Charged cellulose was produced using TEMPO oxidation according to Saito et al.[50] In short, 1 g of CNFs was dispersed in 100 ml of solution, which contained 0.1 mmol of TEMPO and 1 mmol of HBr. The oxidation started when 0.283 g of 12 % NaClO solution that was adjusted to pH 10 with 0.1 M NaOH added (3.8 mmole of NaClO per 1 g of cellulose). The suspension was maintained at pH 10 by adding 0.5 M NaOH dropwise until no NaOH was consumed and the reaction came to an end. TEMPO-oxidized cellulose nanofibers (TCNFs) were purified with dialysis for at least 3 d. The solid content and charge of the TCNFs were measured with a dry matter measurement balance (Mettler Toledo LJ16 with infrared dryer) and a particle charge detector (Mütek™ PCD-02) with polyelectrolyte titration using polydiallyldimethylammonium chloride (polyDADMAC), respectively.

For the adsorption studies described in Paper I, cellulose substrates were prepared using hydroxypropyl cellulose stearate (HPCE) [51] and trimethylsilyl cellulose (TMSC). TMSC and HPCE were dissolved in chloroform at 0.75 wt% and spin-coated on QCM-D and SPR sensors using an acceleration of 2,500 rpm s^{-1} and a speed of 4,000 rpm. TMSC was converted into cellulose by exposing it to HCl vapor for 12 min.

For the adsorption studies described in Paper II, CNF and TCNF films were prepared on commercial SiO_2-coated QCM-D and SPR sensors using the same method. Cleaned sensors were coated with polyethylenimine (PEI) (1.6 g/l) by allowing the PEI to adsorb electrostatically on the surface for 20 min, then rinsing it with water and drying it with N_2. Cellulose suspension (1.7 g cellulose/l suspension) was sonicated with ultrasound in an ice bath for 5 min and centrifuged at 6,000 rpm for 40 min. A clear supernatant was separated and used for spin-coating. To ensure full surface coverage, two layers of cellulose film were coated. The sensors were rinsed and dried like the PEI layer. The films were treated in an oven at 80 °C for 10 min and kept in a desiccator until measurement time.

Phosphate buffer solution (PBS) was used as a mobile phase in the adsorption studies. A liter of PBS contained 1.4 g of $Na_2HPO_4{\cdot}2H_2O$ (8.1 mM), 0.3 g of $NaH_2PO_4{\cdot}H_2O$ (1.9 mM), and 5.8 g NaCl (100 mM). The buffer was adjusted to pH 7.4 with 0.1 M HCl or 0.5 M NaOH.

3.1 Carbohydrate analysis of xylans

The carbohydrate compositions of xylans and oxidized xylan were analyzed using high-performance anion exchange chromatography (HPAEC), and acid hydrolysis was employed for preparation of the samples.[52] In short, xylans and oxidized xylans (0.06 g) were hydrolyzed with 0.6 ml of 72 % H_2SO_4. The hydrolysates were placed in a desiccator connected to a vacuum for 10 min.

Thereafter, they were placed in a water bath at 30 °C for 1 h, followed by dilution with 16.8 ml of deionized water. The hydrolyzed carbohydrates were autoclaved at 120 °C for a further 1 h and filtrated in a vacuum. Filtrates were diluted 20-fold with Milli-Q® water (50 µl sample diluted with 950 µl water), and 50 µl of fucose internal standard was added. The dilutions were then filtered through a 0.2 µm filter. A Dionex ICS-3000 ion chromatography system with pulsed amperometric detection and a CarboPac™ PA1 analytical column was used to detect the carbohydrate type and content.

3.2 Hydrodynamic diameters of oxidized xylans

The hydrodynamic diameters were observed using the dynamic light scattering (DLS) technique. Oxidized xylan solutions were prepared at 0.01 wt% and 0.1 wt% concentrations using PBS buffers rather than solvent. The solutions were filtrated through a 0.45 µm nylon filter before being analyzed using a Nanosizer® ZS90 (Malvern Panalytic, UK). The refractive index of the xylan was determined using a refractometer (Abbemat 550; Anton Paar, Austria). Hydrodynamic diameters (d_H) were calculated from a transitional diffusion coefficient (D) using the Stokes–Einstein equation (Equation 1):

$$d_H = \frac{kT}{3\pi\eta D} \quad (1)$$

Here, k is Boltzmann's constant, T is absolute temperature, and η is viscosity. The number distributions and diffusion coefficients were determined from the autocorrelation function.

3.3 Adsorption of oxidized xylans on model film

3.3.1 QCM-D

The adsorption of oxidized xylans on cellulosic substrate was monitored in situ using QCM-D. The experiment began after obtaining a plateau at the baseline under control conditions (PBS at 22 °C and a flowrate of 100 µl/min), PBS was changed to 0.01wt% oxidized xylan solution for 2 h, then rinsed with PBS.

The adsorbed mass was calculated using the Sauerbrey equation and the viscoelastic model derived by Johannsmann et al.[53] The Sauerbrey equation expresses a linear relationship between mass change (Δm) and frequency shift (Δf) as shown in Equation 2:

$$\Delta m = -C\frac{\Delta f}{n} \quad (2)$$

Here, C is the sensitivity constant of the quartz sensor (0.177 mg/m^2 Hz), n is the overtone number, and n = 1, 3, 5 … 13. For a rigid layer in air or a vacuum, the mass estimated by the Sauerbrey equation would have a similar value for every overtone. When the viscoelastic layer is deposited on the sensor surface in liquid media, the oscillation is dampened by the layer and alters the relationship between Δm and Δf to nonlinear, making the Sauerbrey equation invalid. Cellulose, which is a viscoelastic material, typically requires a modified Sauerbrey equation to account for the viscous property of cellulose. Johannsmann et al. derived a model for viscoelastic material thin film based on equivalent mass ($\widehat{m}^*$) (Equation 3).[53] The equivalent mass of the layer depends on complex shear compliance ($\hat{\jmath}(f)$) at frequency (f). A true mass (m_0) was calculated based on an assumption that $\hat{\jmath}(f)$ is independent of the frequency in the measurement range (Equation 3):[54]

$$\hat{m}^* = m_0\left(1 + \hat{\jmath}(f)\frac{\rho f^2 d^2}{3}\right) \quad 3$$

Here, d is the film thickness. Plotting equivalent mass against frequency squared (f^2) gives true mass as an intercept.

The dissipation factor (D) indicates the structure of the layer on the sensor surface. The viscous property of a material should be included in the estimation, and the energy dissipation during oscillation is described by Equation 4:

$$D = \frac{E_d}{2\pi E_s} \quad 4$$

Here, E_d is energy dissipation during one oscillation and E_s is energy stored in the oscillation system. A small D value implies a rigid structure; in contrast, a soft layer has a larger D value. For viscoelastic film, the material that has a more viscous component shows a larger D value compared to rigid film.

3.3.2 SPR

The same xylan solution conditions and temperature as for QCM-D were used for the SPR analysis of adsorption of oxidized xylan, except that the flowrate was slower (10 µl/min) because of instrument constraints (i.e., the limited injection loop and capacity of the syringe pump). Adsorbed mass (Γ) was calculated using a modified de Feijter equation (Equation 5):

$$\Gamma = \frac{\Delta\Theta\ k\ d_p}{\frac{\mathrm{d}n}{\mathrm{d}c}} \quad 5$$

Here, ΔΘ is a shift of the minimum intensity angular, k is a sensitivity constant of SPR, d_p is the thickness of the adsorbed layer, and dn/dc is a refractive index increment. kd_p can be considered a constant at a specific wavelength when the layer is thinner than 100 nm. The value of kd_p is 0.91×10^{-7} cm/° at 670 nm and 1.56×10^{-7} cm/° at 975 nm.

3.4 Film thickness

Dry thickness was determined using QCM-D. Air was blown through the chamber with the pump set at 100 µl/min flowrate. The thickness was calculated using the Sauerbrey equation, assuming a density ($\rho_{assumed}$) of 1,500 kg/m^3 (Equation 6) [55]:

$$d = \frac{\Delta m}{\rho_{assumed}} \quad 6$$

3.5 Determination of water content in the films

H_2O-D_2O solvent exchange was performed to estimate the amount of water in the film. The experiment was conducted on swollen-state film. A plateau baseline of H_2O was recorded for at least 5 min, then the solvent was changed from H_2O to D_2O and the response was recorded until a plateau in the frequency occurred. Thereafter, the solvent was switched back to H_2O. Calculation of the water contained in the film was based on the advantage of the density difference of H_2O and D_2O (Equation 7).[56] The surface concentration of water in the film (Γ_{water}) was a proportion of the frequency difference between the H_2O and D_2O of water $(\Delta f/n)_{water}$, calculated according to Equation 8:

$$\Gamma_{\text{water}} = -C\left(\frac{\Delta f}{n}\right)_{\text{water}} \quad (7)$$

$$\left(\frac{\Delta f}{n}\right)_{\text{water}} = \frac{\left(\frac{\Delta f}{n}\right)_{\text{film}} - \left(\frac{\Delta f}{n}\right)_{\text{bare}}}{\left(\frac{\rho_{D_2O}}{\rho_{H_2O}}\right) - 1} \quad (8)$$

$(\Delta f/n)_{film}$, $(\Delta f/n)_{bare}$, $\rho_{H_2O,}$ and ρ_{D_2O} are frequency differences between H_2O, the D_2O of the bare sensor and after film coating, the density of H_2O, and the density of D_2O, respectively. C is the sensitivity constant of the quartz sensor, as mentioned previously.

3.6 Film topography

Atomic force microscopy (AFM) was used for imaging the topography of film surfaces. The surface of spin-coated films on QCM-D and SPR sensors was investigated using a NTEGRA AFM (NT-MDT) with NSG01 tips, resonant frequencies of 87–230 kHz, and a force constant of 1.45–15.1 N/m. At least four different positions on the surface were imaged.

4. Results and Discussion

4.1 Characterization of oxidized xylans

Established methods for determining the DO of polysaccharides include the analysis of DO during oxidation or of the product.[43] Here, the DO could be determined directly by tracing periodate consumption during oxidation using UV-Vis spectroscopy.[57] A periodate ion (IO_4^-) has a characteristic peak at 290 nm, which reduces in intensity when the IO_4^- ions are converted to IO_3^- and vanishes when all IO_4^- ions are consumed. Absorbance intensity at 290 nm was converted to a concentration of periodate ion and used to study the kinetics of the reaction and the DO. The DO for the xylan grades used for the adsorption studies described in Paper II were 91.6 % and 91.7 % for HX and LX, respectively. Efforts to oxidize xylan to various DOs (currently under investigation) revealed a few characteristics of UV-absorbance-based DO determination. The literature reported straightforward observation of absorbance at 290 nm and correlations to calibrations with aqueous $NaIO_4$ solutions. However, during the periodate oxidation of xylan, it became evident that an absorbance intensity could not always be translated to DO directly because xylan contributed to the absorbance. In the case of most cellulose materials, this is not a problem, since the fibers or particles can be removed via filtration. However, filtration could not remove xylan completely, which hindered the DO determination. This obstacle was overcome by not filtering the solutions and instead subtracting the signal from the xylan background on the assumption that the xylan background was not affected by the oxidation. However, the solubility of the xylan in the system should vary with the DO; hence, the UV-absorbance-based DO determination requires further investigation.

We introduced a complementary way of confirming that the DO was based on carbohydrate composition, and we suggested an indirect method of determining DO for carbohydrates. The method was initially introduced by Börjesson et al.[44], and we developed it further. The hypothesis was that oxidation cleaves the carbon bond at C2–C3 and opens the cyclic structure of carbohydrates. When these saccharides are exposed to acid hydrolysis, they are degraded and cannot be detected; hence, only the composition of the intact carbohydrates should be recorded. The carbohydrate composition analysis revealed that the amount of total carbohydrate decreased dramatically from 90 % to 7 % in the case of HX and 91 % to 5 % in LX after oxidation (Table 1). A reduction of detected carbohydrates corresponded to the DO defined by UV -Vis spectroscopy. Under the assumption that all the lost carbohydrates were oxidized, the DO values determined by the carbohydrate analysis were 93 % and 95 % DO for HX and LX, respectively. These values were close to the DO of 92 % determined using UV absorbance at 290 nm. Carbohydrate analysis is therefore suggested as a complementary method for the DO determination of hemicelluloses.

Table 1. Carbohydrate composition of unoxidized and oxidized xylans. Original published in Palasingh et al.[58], licensed under CC BY 4.0.

Sample/Grade	%weight					
	Arabinose	Galactose	Glucose	Xylose	Mannose	Total
Unoxidized HX	0.7	0.0	0.8	**88.9**	0.0	90.4
Unoxidized LX	0.2	0.0	1.7	**89.3**	0.0	91.1
Oxidized HX	0.7	0.0	0.0	**6.1**	0.0	6.8
Oxidized LX	1.1	0.0	0.0	**4.3**	0.0	5.4

The hydrodynamic diameters of oxidized xylans were reported in Paper II, with the investigations done in a buffer solution and determined using DLS. It measures particles diffusing

due to Brownian motion and translates it to hydrodynamic diameter through the intensity of scattered light. Brownian motion is influenced by particle size; large particles move more slowly and have slower Brownian motion than small particles. A correlation curve is constructed by comparing the similarity of intensity of a signal (scattered light) at time zero to a signal at various other times and translating the similarity into a coefficient. A correlation coefficient ranges from 1 (perfect correlation) to 0 (no correlation), with a starting value relating to a useful signal in the measurement. Delays in the correlation function relate to particle size. Large particles move more slowly than small ones, as shown in Figures 5a and 5b, where LX decayed faster than HX. A plateau in Figure 5b was evidence of a second population in the LX sample.

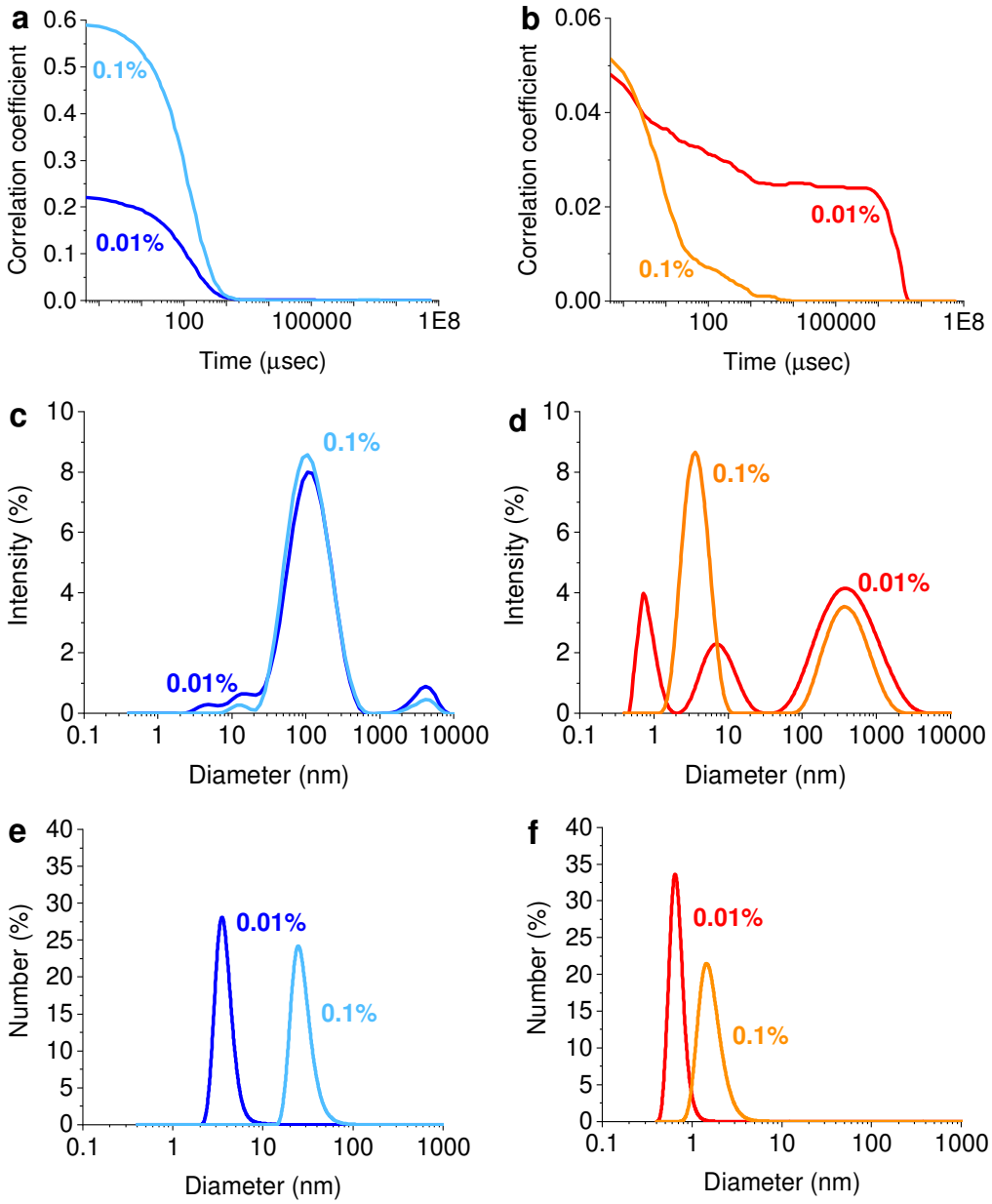

Figure 5. Autocorrelation curves (a and b), size distribution by intensity (c and d), and size distribution by number (e and f) of oxidized HX (left) and oxidized LX (right) dispersed in PBS buffer at concentrations of 0.1 and 0.01 wt% at 22°C. Adapted from Palasingh et al.[58], licensed under CC BY 4.0.

Moreover, the polydispersity of oxidized LX and HX was verified by the intensity size distribution, in which various sizes of particles were detected (Figure 5c and 5d). By inputting a refractive index, intensity size distributions can be translated into number size distributions. The hydrodynamic size increased as the concentration of oxidized xylans increased in number size distribution (Figure 5e and 5f). The mean diameters of oxidized HX and LX were approximately 3.6 nm and 0.6 nm for 0.01 wt% and 24.4 nm and 1.5 nm for 0.1 wt%, respectively.

4.2 Using model films to study the adsorption of macromolecules

Model films that are less than 100 nm thick are referred to the film materials used in specific analyses as substrates to mimic the properties of the material being investigated. In general, there are two types of model films—open and closed—with open film referring to material islands on a substrate or isolated particles on a substrate, and closed film referring to a film where the material fully covers the substrate.[59, 60] Open films are suitable for studying particle size or individual particle interaction, while closed films are used to study adsorption, swelling, and the surface energy of areas. The films are typically prepared by spin-coating using Langmuir–Blodgett drought, Langmuir–Schaeffer deposition, or drop casting.[27, 59, 60] In this study, closed model films of celluloses and xylans were prepared by spin-coating for QCM-D and SPR analyses, which is a common method of producing closed films. Furthermore, substrate material plays an important role in the production of fully covered films (e.g., cellulose films can be spin-coated on mica, silicon wafer, and QCM, and SPR sensors with Au or SiO_2 surfaces). An adhesion layer may be required when the material does not spread to fully cover the substrate film. As described in Paper II, heat treatment after film deposition improved film stability, which is especially important for studies conducted in aqueous environments.

For Paper I, cellulose model films were prepared using the cellulose derivatives TMSC and HPCE, which dissolve in chloroform and can be spin-coated as a solution. TMSC can be exposed to HCl vapor to desilylate and convert to cellulose.[59] The purpose of using cellulose solutions to prepare cellulose films is to generate uniform films with chemical equivalence to cellulose and avoid morphology stemming from cellulose particles. However, the use of fibrils (as in Paper II) offers a way to also include the parameter of the fibrillar structure of cellulose in adsorption studies. The cellulose derivatives for Paper II were spin-coated to form one-component films but also blended and spin-coated to form blend films. The blends resulted in spinodal decomposition that enabled the preparation of films with protrusions and cavities in a matrix. Such model films are an interesting subject for future studies on the adsorption of macromolecules on cellulose surfaces. For Paper I, a surface fraction of 37 % cellulose in HPCE exhibited outlier adsorption inhibiting macromolecule adsorption. The underlying reasons may be surface energy, roughness, or surface configuration, and they remain to be investigated in future studies.

4.3 Adsorption of oxidized xylans on cellulose films

The adsorption mechanism involves the concentration of moieties near the surface. The tendency of polymers to aggregate in a solution, as well as their overall solubility, depends on the molecular weight of polymers. The polymer chain length has an entropic preference to the adsorption. Even if a surface has equal affinity with different chain lengths, entropy decreases strongly with longer molecules, which is preferable for the system. Moreover, longer molecules, which have multiple anchor segments and are likely to form loops and tails, have advantages over the adsorption of small molecules.[61] The hydrodynamic radius of the HX increased 6.8-fold, while the increase for LX was 2.5-fold when increasing the concentration from 0.01 to 0.1 wt%. This showed that HX is prone to self-aggregate at lower concentrations compared to LX.

The Sauerbrey equation is applicable for the analysis of adsorbed mass for rigid materials that do not exhibit high dissipation. Cellulose films contain water and hence are expected to be dissipative. One way to evaluate this is to observe the dependence of the adsorbed mass on the overtones; indeed, here the calculated adsorbed mass was overtone-dependent and provided evidence of the viscoelastic property of the CNF films (Figure 6). The challenge of the Sauerbrey equation can be overcome by utilizing the Johannsmann approach to calculating the adsorbed mass, which accounts for the viscoelastic property of films.[53]

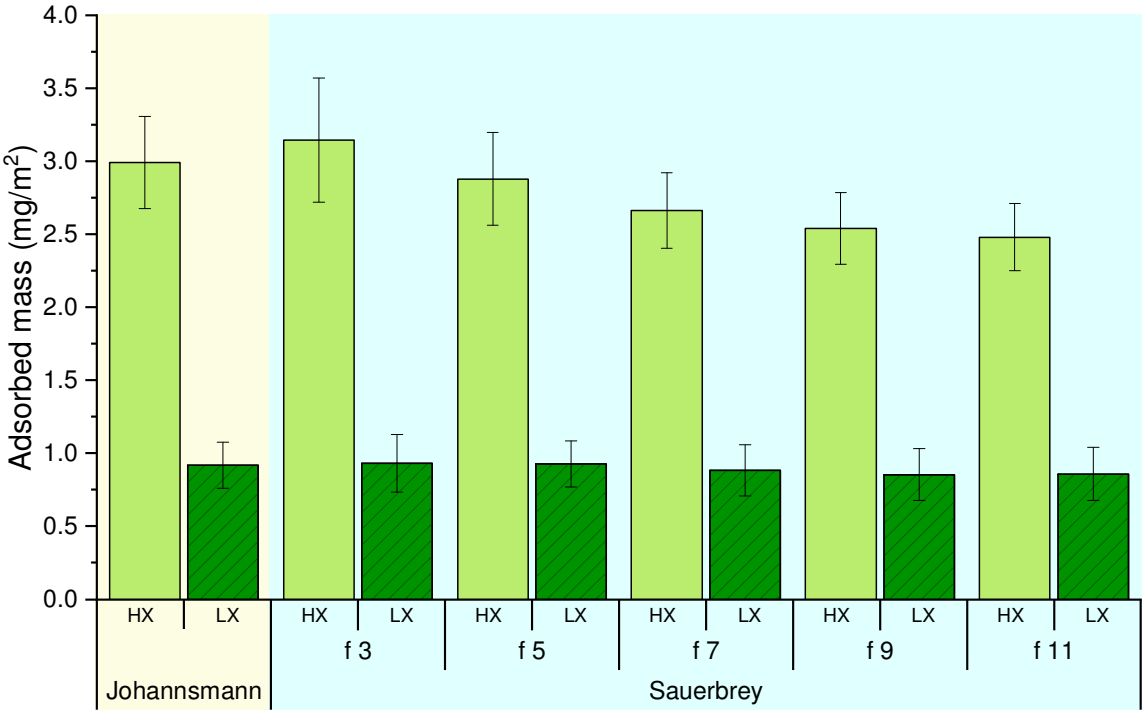

Figure 6. Adsorbed mass of the oxidized high molecular weight xylan on CNF film as defined by the Johannsmann and Sauerbrey equations. Original published in Palasingh et al.[58], licensed under CC BY 4.0.

A difference in adsorbed mass between QCM-D and SPR is mainly due to the capability of the equipment to identify the adsorbing polymer from the solvent interacting with the substrate. QCM-D detects resonance frequency changes of the total mass on a surface; the adsorbed amount is the sum of the adsorbent and the water bound to the adsorbing film. By contrast, adsorbed mass calculated using the SPR response is based on refractive index increments (Equation 5) and allows calculation of only adsorbent mass.

The experiments were divided into two systems: adsorption of an uncharged polymer on a neutral surface and adsorption of an uncharged polymer on a charged surface. For the first case, the HX grade resulted in a larger amount adsorbed mass on the CNF surfaces, a closer to neutral charged surface, than the LX grade (Figure 7). The main reason was likely to be the molecular weight. Molecular weight influences solubility, which contributes to adsorption. Furthermore, from an entropy perspective, HX adsorption on the surface was more entropy favorable than LX adsorption because of the higher molecular weight. In the latter system, a negatively charged surface was produced with oxidized cellulose by converting the hydroxyl group at C6 to a carboxylate (TCNFs). The charge was -409.58 μeq/g after the oxidation, which was a higher negative charge than the initial

charge (-35.51 μeq/g). The adsorbed amount based on the QCM-D of the HX was less than the adsorption on the CNF layer. LX adsorbed a similar amount to CNF film. The advantage of the molecular weight of HX was no longer pronounced, probably due to competition between counterions and oxidized xylans. They competed for space on the surface while the surface maintained its electroneutrality and entropy gain from the adsorption. Moreover, carboxylate groups promote water binding. This can obstruct entropy-driven adsorption, as in the case of HX.

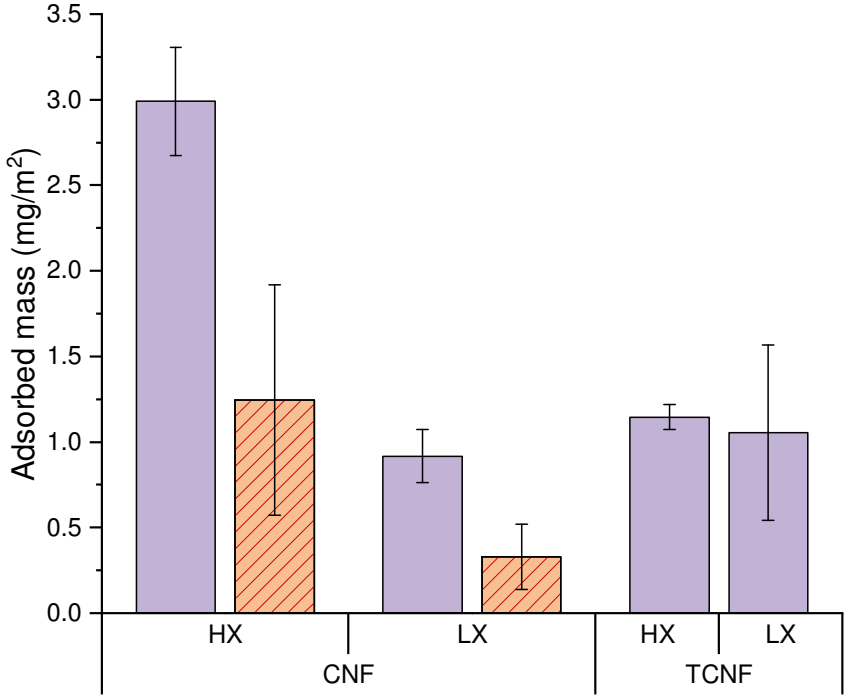

Figure 7. Adsorbed mass of high and low molecular weight oxidized xylan on CNF and TCNF films using QCM-D ( ) and SPR ( ). Original published in Palasingh et al.[58], licensed under CC BY 4.0.

Plotting dissipation against changes in frequency obtained from the QCM-D gave an idea of the viscoelastic property of the adsorbing layer during adsorption and of adsorption kinetics (Figure 8). The amount of adsorbed mass, including water, correlated with the magnitude of a frequency change. Those two species contribute to changes in dissipation. An increase in dissipation implies an increase in the viscous behavior of the layer. In our system, this could be a contribution of a looser cellulose network due to swelling of the layer and the association of water in the layer. The latter was most likely because water could be brought to the layer by the oxidized xylan. The slope of $\Delta D/\Delta f$ indicated a change in the viscoelastic property of the film, and a high value indicated that the viscous component increased more than the elastic component. For the HX adsorbed on the CNF film, which had a steeper slope than the LX on the same film, a portion of the viscous component increased more than the elastic component, resulting in a more swollen film. This agreed with the larger hydrodynamic diameter findings obtained with DLS; larger particle size could bring more water with it. In the case of the layer accumulating on the TCNF film, the level of hydration increased faster with respect to mass increases than on the CNF substrate. This supported the observation that the layers on TCNFs are more hydrated. The $\Delta D/\Delta f$ curve for the LX adsorption on TCNFs revealed a change in the slope with the first higher rate of uptake of water. This tendency was opposite to the adsorption on CNFs, where the mass increased faster than the dissipation. The density of data points gave an idea of the adsorption rate, since each data point was measured with a constant time interval. HX

adsorbed rapidly at the beginning of the adsorption on the CNF film, then slowed down until the end of the experiment. LX adsorbed more slowly and uniformly during the measurement time. Moreover, the system did not reach a plateau after 2 h of adsorption time regardless of the surfaces and molecular weights of oxidized xylan used. This was a general tendency for all the grades and an indication of an intrinsic characteristic of natural polysaccharides that are likely to come with high polydispersity rather than a defined molecular weight when no fractionation is applied. This suggested that oxidized xylans were polydispersed, which supported the DLS results. Small molecules diffuse across a surface faster and adsorb first, then the larger molecules reach the surface and eventually displace small ones when the surface is saturated; hence, polydispersed solutions take longer to reach an adsorption plateau.[62]

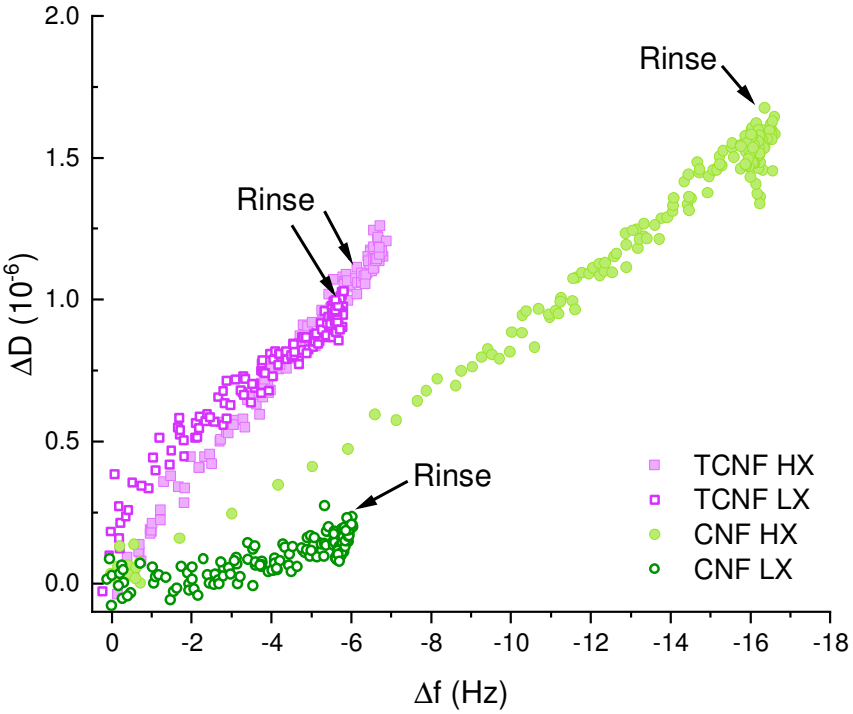

Figure 8. A change in dissipation (ΔD) versus a change in frequency (Δf) of the seventh overtone upon adsorption of high and low molecular weight oxidized xylan on CNF and TCNF films. Original published in Palasingh et al.[58], licensed under CC BY 4.0.

Film thickness in the QCM-D experiments required film density to convert adsorbed mass per area to thickness. The dry CNF films were thicker than those of TCNF films (Figure 9), perhaps due to ionic repulsion of charged TCNF fibrils leading to well dispersed fibrils in a suspension, consequently generating a thinner film.[62] Film thickness changed slightly after oxidized xylan adsorption in all cases, but the changes were statistically insignificant in the case of LX adsorption on CNF and TCNF films. A minor change in thickness could be caused by contamination when the sensor had to be removed during the measurement, especially for thin film, potentially leading to large deviations. We attempted to use a profilometer to determine film thickness; however, films needed to be scratched to observe the height profile of the layer, which was not suitable for films on QCM-D and SPR sensors that the sensors would be damaged by scratching. Nevertheless, this technique is a fast and useful measure for determining thin film thickness on some substrates (e.g., standard silicon substrates) but not sensors.

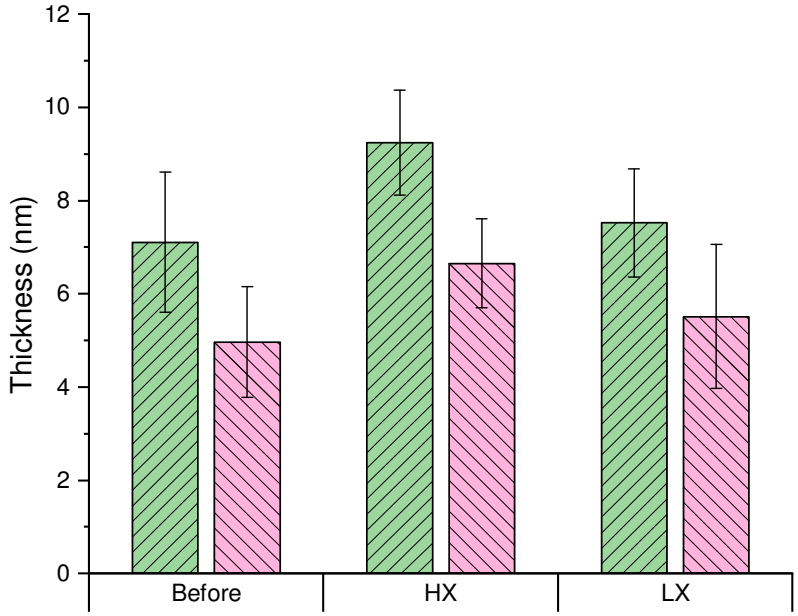

Figure 9. Film *thickness of CNF ( ) and TCNF ( ) films determined using QCM-D at different resonance frequencies in air. Original published in Palasingh et al.[58], licensed under CC BY 4.0.*

The topography of the film surface showed no significant difference after adsorption of each xylan grade (Figure 10). No oxidized xylan aggregates were detected on the surface. Eronen et al. reported similar results with polysaccharide adsorption on CNF films, showing no changes in substrate morphologies after adsorption.[63]

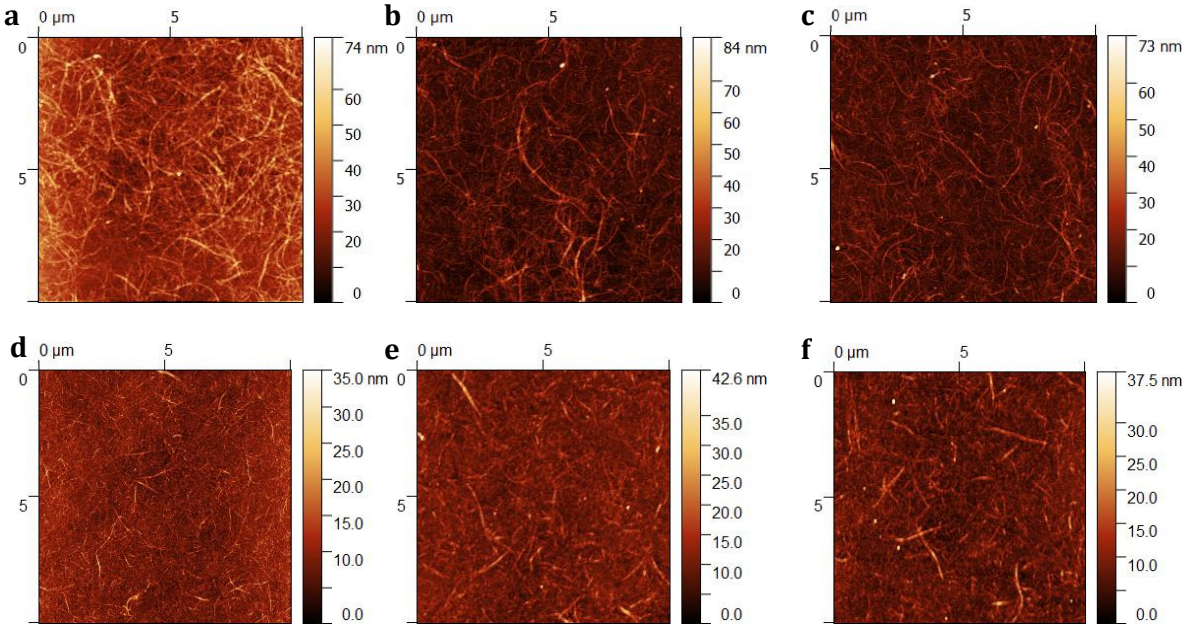

Figure 10. Surface topography of CNF film before (a) and after the adsorption of high molecular weight (b) and low molecular weight (c). TCNF film before (d) and after high molecular weight (e) and low molecular weight (f) adsorption. Original published in Palasingh et al.[58], licensed under CC BY 4.0.

4.4 Water content of thin films

Celluloses and hemicelluloses are generally hygroscopic materials, and their behavior is often determined by humidity and moisture content. At high humidity, they tend to perform poorly due to water penetration and weakening component interactions. As explained in Paper I, the hydrophilicity of cellulose played an important role in protein adsorption. Since adsorption in aqueous conditions is a process governed by entropy, an entropy loss from adsorbed molecules or polymers has to be compensated for by entropy gain in other parts of the system. When molecules or polymer segments are adsorbed onto a surface, the balance is disturbed, and the surface will maintain the balance by releasing ions or water. In Paper I, bovine serum albumin (BSA) deposition involves the replacement of water close to the BSA molecules and cellulose surface; this led to poorly BSA adsorption performance on hydrated cellulose due to entropically unfavorable conditions. The hydrophobic cellulose derivative HPCE was used to alter the protein adsorption behavior by reducing the water content in the cellulose–HPCE blend film and enhancing BSA adsorption.

As described in Paper II, observations of swollen state cellulose films were conducted using QCM-D with solvent exchange between water and deuterated water. An amount of water in the film could be extracted due to the difference in density of H_2O and D_2O. Water molecules not only couple on a surface, but can also penetrate into the film through pores or free space between fibrils to some depth. Kittle et al. reported that the water in film is proportional to the film's thickness.[56] Since TCNF film was approximately 30 % thinner than CNF film, thickness or dry matter had to be taken into account when analyzing the adsorbed water (Figure 11). Compared to CNF film, TCNF films contained more water due to electrostatic repulsion between carboxylate groups and the interaction of counterions, which promoted swelling.[64] Adsorption of HX and LX increased the water in the CNF film. Oxidized xylans brought water, and HX brought slightly more water, which was a consequence of its larger hydrodynamic diameter. By contrast, the amount of water in the TCNF film decreased after oxidized xylan adsorption. Adsorbed LX had the least amount of water, since osmotic pressure and swelling pressure governed swelling and oxidized xylans replaced counterions on the TCNF film, leading to a decrease of osmotic pressure and, consequently, less associated water in the film and condensed on the film.

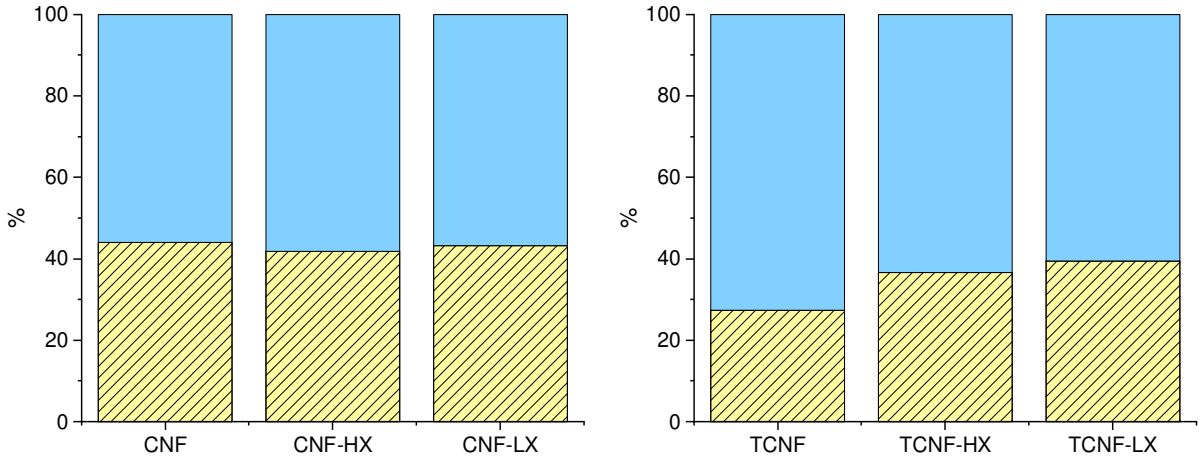

Figure 11. Amounts and percentages of film materials (▨) and water (▭) on CNF (left) and TCNF (right) films for the seventh overtone. The film mass was calculated using the Sauerbrey equation, and the water amount was determined according to Kittle et al.'s method.[56] Original published in Palasingh et al.[58], licensed under CC BY 4.0.

Since SPR does not determine water in the film mass, a difference between adsorbed mass extracted from SPR and QCM-D was considered to reflect the amount of water in a film. HX adsorbed on the CNF film contained 1.74 mg/m^2 of water in a swollen state and LX adsorbed on the CNF film contained 0.59 mg/m^2. This subtraction method complied with the water content trend observed using the solvent exchange method.

5. Conclusions and Outlook

This research demonstrated that oxidation renders solubility, leading to adsorption of xylans on cellulose. Solvent interactions are an underlying challenge for xylan polymer utilization, and indeed, since the starting xylans were not water-soluble, the oxidation led to a water solution that could be used for addition by adsorption.

The aim was to reveal the properties of oxidized xylan in solution and its influence on polysaccharide films when used as an additive. The study indicated that the water content in cellulose films can be altered by xylan adsorption. The benefit of the oxidized xylans in the cellulose materials was shown to be reduced water content in TCNFs. While the water reduction seemed modest as an absolute value, it needed to be considered in the context of the pulp and paper industry for which these materials are relevant. Any decrease in water content leads to a magnified effect on the production of materials that is dominated by the process of drying via evaporation.

This work investigated the influence of the molecular weight of oxidized xylans with 92 % Degree of oxidation (DO), resulting in slightly different adsorbed mass and swelling behavior. To simplify the system and obtain a clearer view, oxidized xylan films will be used for future studies. However, preliminary experiments on 92 % DO oxidized xylan film found that the model films were smooth and homogeneous but were not stable in water due to their high water solubility. The next step toward utilization would be to link the DO to solubility and possibly to film formation. An optimal DO to enable xylan to dissolve in water and form a stable film needs to be investigated to produce films that can be used in QCM-D and SPR experiments and minimize production costs. Unoxidized xylan conformation in solution cannot be translated without doubt to the derivative with opened rings in high DO; hence, the findings of this research are paramount for elucidating the properties of this water-interacting derivative. Further research on oxidized xylan in solution—its conformation and behavior—could be conducted using DLS and, if possible, neutron scattering. QCM-D and SPR will be used to study the swelling and stability of oxidized xylan films in different pH environments.

6. Acknowledgements

This thesis was funded by a Swedish Research Council grant 2017-05138. I would like to express gratitude to the people who supported me throughout this study; this thesis could not have been completed without their help. I would like to give special thanks to my supervisors, Tiina Nypelö and Anna Ström, for their support, guidance, and wisdom, and to Hanna Härelind, my examiner. Sincere thanks go to the people in the Larsson-Ström-Nypelö group for their support; Aline Maire Du Poset (our former colleague) for assistance with the UV-Vis spectroscopy and oxidation, Anette Larsson for help in analyzing the UV-Vis data, Parveen Kumar Deralia and Kenneth Gacutno Arandia for the HPAEC, Gustav Ferrand-Drake Del Castillo for the SPR, Mats Hulander for the QCM-D, Romain Bordes for sharing cellulose material, and Hassan Amer for filling in missing information. Last but not least, I thank my family and friends for supporting, caring for, and encouraging me.

7. References

1. Ek, M., G. Gellerstedt, and G. Henriksson, The Worldwide Wood Resource, in Pulp and Paper Chemistry and Technology - Wood Chemistry and Biotechnology, Volume 1. 2009, De Gruyter, Inc.: Berlin/Boston, GERMANY.
2. Mathew, A.K., et al., Chapter 9 - Lignocellulosic Biorefinery Wastes, or Resources?, in Waste Biorefinery, T. Bhaskar, et al., Editors. 2018, Elsevier. p. 267-297.
3. Ebringerová, A., Structural Diversity and Application Potential of Hemicelluloses. Macromolecular Symposia, 2005. **232**(1): p. 1-12.
4. Spiridon, I. and V.I. Popa, Chapter 13 - Hemicelluloses: Major Sources, Properties and Applications, in Monomers, Polymers and Composites from Renewable Resources, M.N. Belgacem and A. Gandini, Editors. 2008, Elsevier: Amsterdam. p. 289-304.
5. Bozdemir, Ö.A. and M. TUTAŞ, Plasticiser Effect on Water Vapour Permeability Properties of Locust bean gum-Based Edible Films. Turkish Journal of Chemistry, 2003. **27**(6): p. 773-782.
6. Ruelas-Chacon, X., et al., Guar Gum as an Edible Coating for Enhancing Shelf-Life and Improving Postharvest Quality of Roma Tomato (Solanum lycopersicum L.). Journal of Food Quality, 2017. **2017**.
7. Miletzky, A., et al., Modifying Cellulose Fibers by Adsorption/precipitation of Xylan. Cellulose, 2015. **22**(1): p. 189-201.
8. Henriksson, Å. and P. Gatenholm, Controlled Assembly of Glucuronoxylans onto Cellulose Fibres. Holzforschung, 2001. **55**(5): p. 494-502.
9. Prakobna, K., et al., Strong Reinforcing Effects from Galactoglucomannan Hemicellulose on Mechanical Behavior of Wet Cellulose Nanofiber Gels. Journal of Materials Science, 2015. **50**(22): p. 7413-7423.
10. Tanaka, R., et al., Viscoelastic Properties of Core–Shell-Structured, Hemicellulose-Rich Nanofibrillated Cellulose in Dispersion and Wet-Film States. Biomacromolecules, 2016. **17**(6): p. 2104-2111.
11. Gröndahl, M., et al., Polymeric Film or Coating Comprising Hemicellulose. 2013, Google Patents: USA.
12. Gröndahl, M., L. Eriksson, and P. Gatenholm, Material Properties of Plasticized Hardwood Xylans for Potential Application as Oxygen Barrier Films. Biomacromolecules, 2004. **5**(4): p. 1528-1535.
13. Hansen, N.M.L., et al., Properties of Plasticized Composite Films Prepared from Nanofibrillated Cellulose and Birch Wood Xylan. Cellulose, 2012. **19**(6): p. 2015-2031.
14. Hartman, J., et al., Oxygen Barrier Materials from Renewable Sources: Material Properties of Softwood Hemicellulose-based Films. Journal of Applied Polymer Science, 2006. **100**(4): p. 2985-2991.
15. Hartman, J., A.C. Albertsson, and J. Sjöberg, Surface- and Bulk-modified Galactoglucomannan Hemicellulose Films and Film Laminates for Versatile Oxygen Barriers. Biomacromolecules, 2006. **7**(6): p. 1983-1989.
16. Kisonen, V., et al., O-acetyl Galactoglucomannan Esters for Barrier Coatings. Cellulose, 2014. **21**(6): p. 4497-4509.
17. Dalvi, L.C., et al., Study of Xylan and Cellulose Interactions Monitored with Solid-state NMR and QCM-D. Holzforschung, 2019.
18. Jaafar, Z., et al., Meaning of Xylan Acetylation on Xylan-cellulose Interactions: A Quartz Crystal Microbalance with Dissipation (QCM-D) and Molecular Dynamic Study. Carbohydrate Polymers, 2019. **226**: p. 115315.
19. Köhnke, T., Å. Östlund, and H. Brelid, Adsorption of Arabinoxylan on Cellulosic Surfaces: Influence of Degree of Substitution and Substitution Pattern on Adsorption Characteristics. Biomacromolecules, 2011. **12**(7): p. 2633-2641.

20. Köhnke, T., et al., The Effect of Barley Husk Arabinoxylan Adsorption on The Properties of Cellulose Fibres. Cellulose, 2008. **15**(4): p. 537-546.
21. Mikkonen, K.S., et al., Arabinoxylan Structure Affects The Reinforcement of Films by Microfibrillated Cellulose. Cellulose, 2012. **19**(2): p. 467-480.
22. Kabel, M.A., et al., Structural Differences of Xylans Affect Their Interaction with Cellulose. Carbohydrate Polymers, 2007. **69**(1): p. 94-105.
23. Paananen, A., et al., Interaction between Cellulose and Xylan: An Atomic Force Microscope and Quartz Crystal Microbalance Study, in Hemicelluloses: Science and Technology. 2004, American Chemical Society. p. 269-290.
24. Amer, H., et al., Synthesis and Characterization of Periodate-oxidized Polysaccharides: Dialdehyde Xylan (DAX). Biomacromolecules, 2016. **17**(9): p. 2972-2980.
25. Ek, M., G. Gellerstedt, and G. Henriksson, Cellulose and Carbohydrate Chemistry, in Pulp and Paper Chemistry and Technology - Wood Chemistry and Biotechnology, Volume 1. 2009, De Gruyter: Berlin/Boston, GERMANY.
26. Sjöström, E., Wood Polysaccharides, in Wood Chemistry, E. Sjöström, Editor. 1993, Academic Press: San Diego. p. 51-70.
27. Ahola, S., et al., Model Films from Native Cellulose Nanofibrils. Preparation, Swelling, and Surface Interactions. Biomacromolecules, 2008. **9**(4): p. 1273-1282.
28. Nechyporchuk, O., M.N. Belgacem, and J. Bras, Production of Cellulose Nanofibrils: A Review of Recent Advances. Industrial Crops and Products, 2016. **93**: p. 2-25.
29. Salas, C., et al., Nanocellulose Properties and Applications in Colloids and Interfaces. Current Opinion in Colloid and Interface Science, 2014. **19**: p. 383-396.
30. Arrieta, M.P., et al., Chapter 7 - Nanocellulose-based Polymeric Blends for Food Packaging Applications, in Multifunctional Polymeric Nanocomposites Based on Cellulosic Reinforcements, D. Puglia, E. Fortunati, and J.M. Kenny, Editors. 2016, William Andrew Publishing. p. 205-252.
31. Hubbe, M.A., et al., Nanocellulose in Thin Films, Coatings, and Plies for Packaging Applications: A Review. BioResources, 2017. **12**(1): p. 2143-2233.
32. El Seoud, O.A., et al., Cellulose Swelling by Protic Solvents: Which Properties of The Biopolymer and The Solvent Matter? Cellulose, 2008. **15**(3): p. 371-392.
33. Ek, M., G. Gellerstedt, and G. Henriksson, Hemicelluloses and Pectins, in Pulp and Paper Chemistry and Technology - Wood Chemistry and Biotechnology, Volume 1. 2009, De Gruyter: Berlin/Boston, GERMANY.
34. Koch, G., Raw Material for Pulp, in Handbook of Pulp. 2006, WILEY-VCH. p. 21-68.
35. Bouveng, H.O., P.J. Garegg, and B. Lindberg, Position of O-acetyl Groups in Birch Xylan. Acta Chemica Scandinavica, 1960. **14**: p. 742-748.
36. Puls, J., et al., Products of Hydrolysis of Beechwood Acetyl-4-O-methylglucuronoxylan by A Xylanase and An Acetyl Xylan Esterase. Enzyme and Microbial Technology, 1991. **13**(6): p. 483-486.
37. Teleman, A., et al., Characterization of O-acetyl-(4-O-methylglucurono) Xylan Isolated from Birch and Beech. Carbohydrate Research, 2002. **337**(4): p. 373-377.
38. Sixta, H., A. Potthast, and A.W. Krotschek, Chemical Pulping Processe: Sections 4.1-4.2, in Handbook of Pulp, H. Sixta, Editor. 2006, WILEY-VCH. p. 109-229.
39. Gröndahl, M., A. Teleman, and P. Gatenholm, Effect of Acetylation on The Material Properties of Glucuronoxylan from Aspen Wood. Carbohydrate Polymers, 2003. **52**(4): p. 359-366.
40. Hettrich, K., et al., Preparation and Characterization of Water-soluble Xylan Ethers. Polymers, 2017. **9**(4): p. 129.
41. Laine, C., et al., Hydroxyalkylated Xylans – Their Synthesis and Application in Coatings for Packaging and Paper. Industrial Crops and Products, 2013. **44**: p. 692-704.

42. Sharon, N., Complex Carbohydrates, Their Chemistry, Biosynthesis, and Functions. 1975, Massachusetts, United States of America: Addison-Wesley 258-281.
43. Nypelö, T., et al., Periodate Oxidation of Wood Polysaccharides–Modulation of Hierarchies. Carbohydrate Polymers, 2020: p. 117105.
44. Börjesson, M., et al., Periodate Oxidation of Xylan-based Hemicelluloses and Its Effect on Their Thermal Properties. Carbohydrate polymers, 2018. **202**: p. 280-287.
45. PubChem Compound Summary for CID 23667635, Sodium periodate. [cited 2021 January 18]; Available from: https://pubchem.ncbi.nlm.nih.gov/compound/Sodium-periodate
46. Liimatainen, H., et al., Regeneration and Recycling of Aqueous Periodate Solution in Dialdehyde Cellulose Production. Journal of Wood Chemistry and Technology, 2013. **33**(4): p. 258-266.
47. Koprivica, S., et al., Regeneration of Aqueous Periodate Solutions by Ozone Treatment: A Sustainable Approach for Dialdehyde Cellulose Production. ChemSusChem, 2016. **9**(8): p. 825-33.
48. Merwe, P.A., Surface PlasmonRresonance. 2002. p. 1-4.
49. Maekawa, E., T. Kosaki, and T. Koshijima, Periodate Oxidation of Mercerized Cellulose and Regenerated Cellulose, in Wood Research Institute 1986, Kyoto University. p. 44-49.
50. Saito, T., et al., Cellulose Nanofibers Prepared by TEMPO-mediated Oxidation of Native Cellulose. Biomacromolecules, 2007. **8**(8): p. 2485-2491.
51. Nau, M., D. Seelinger, and M. Biesalski, Functional surface coatings from tailor-made long-chain hydroxypropyl cellulose ester nanoparticles. Cellulose, 2018. **25**(10): p. 5769-5780.
52. Theander, O. and E.A. Westerlund, Studies on Dietary Fiber. 3. Improved Procedures for Analysis of Dietary Fiber. Journal of Agricultural and Food Chemistry, 1986. **34**(2): p. 330-336.
53. Johannsmann, D., et al., Viscoelastic Properties of Thin Films Probed with A Quartz-crystal Resonator. Physical Review B, 1992. **46**(12): p. 7808-7815.
54. Naderi, A. and P.M. Claesson, Adsorption Properties of Polyelectrolyte− Surfactant Complexes on Hydrophobic Surfaces Studied by QCM-D. Langmuir, 2006. **22**(18): p. 7639-7645.
55. Tammelin, T., et al., Correlation between Cellulose Thin Film Supramolecular Structures and Interactions with Water. Soft Matter, 2015. **11**(21): p. 4273-4282.
56. Kittle, J.D., et al., Equilibrium Water Contents of Cellulose Films Determined via Solvent Exchange and Quartz Crystal Microbalance with Dissipation Monitoring. Biomacromolecules, 2011. **12**(8): p. 2881-2887.
57. Malaprade, L., Oxidation of Some Polyalcohols by Periodic Acid—Applications. Comptes Rendus, 1928. **186**: p. 382-384.
58. Palasingh, C., et al., Oxidized Xylan Additive for Nanocellulose Films – A Swelling Modifier. International Journal of Biological Macromolecules, 2021. **180**: p. 753-759.
59. Kontturi, E., T. Tammelin, and M. Österberg, Cellulose—Model Films and the Fundamental Approach. Chemical Society Reviews, 2006. **35**(12): p. 1287-1304.
60. Foster, E.J., et al., Current Characterization Methods for Cellulose Nanomaterials. Chemical Society Reviews, 2018. **47**(8): p. 2609-2679.
61. Fleer, G., et al., Polymers at Interfaces. 1993: Springer Science and Business Media.
62. Fall, A.B., et al., Colloidal stability of aqueous nanofibrillated cellulose dispersions. Langmuir, 2011. **27**(18): p. 11332-11338.
63. Eronen, P., et al., Interactions of Structurally Different Hemicelluloses with Nanofibrillar Cellulose. Carbohydrate Polymers, 2011. **86**(3): p. 1281-1290.
64. Chang, C., et al., *Swelling Behaviors of pH- and Salt-responsive Cellulose-based Hydrogels.* Macromolecules, 2011. **44**(6): p. 1642-1648.